Coupling-induced resonance in two mutually and asymmetrically coupled oscillators

Thomas W. Carr*
Department of Mathematics, Southern Methodist University, Dallas, Texas 75275-0156, USA
(Received 5 May 2008; published 18 August 2008)

We consider two mutually coupled oscillators, where we have independent control over the magnitude, sign, and delay of the coupling signal. For appropriate tuning of the coupling constants, there is a coupling-induced resonance where the amplitude becomes large. We investigate the role of nonlinear dissipation and amplitude-dependent frequency correction on the coupling resonance. With delayed coupling, we track the deformation of the resonant bifurcation equation through imperfect bifurcations and the generation of isolas, which generate intervals of multistability between oscillations of different amplitudes. The resonance should be observable in coupled-oscillator systems, where the amplitude remains an important dynamical variable, but not in limit-cycle oscillators modeled by phase-only descriptions.

DOI: 10.1103/PhysRevE.78.026207 PACS number(s): 05.45.Xt, 02.30.Hq, 02.30.Ks, 02.30.Oz

I. INTRODUCTION

In recent theoretical work on two mutually coupled lasers [1], we reported on the existence of an amplitude resonance that occurs for weak coupling. That is, the coupling constants may be tuned such that the amplitude of periodic oscillations, generated via a Hopf bifurcation, becomes large; for values of the coupling tuned away from the resonance, the amplitude of the periodic oscillations is small. In [2] we found that this resonance phenomenon also exists for two coupled lasers with delay and possesses parameter regions where there is bistability. In the present paper we address two unresolved issues from our earlier work. First, in [1] our analysis could identify the coupling values when the amplitude resonance occurred, but the bifurcation equation was singular in that it predicted unbounded amplitudes; here, we show that the amplitude-dependent phase is the source of the resonance, while higher-order nonlinear dissipation is sufficient to remove the singularity that appears in the leading-order result. Second, in [2] we did not track the continuous deformation of the bifurcation curves as the parameters were varied; in this paper, we track disconnected branches of solutions and find imperfect bifurcations and isolas of the periodic oscillations. While our investigations were originally motivated by the dynamics of lasers, and we will again use the laser model as a convenient starting point, the results follow from quite generic normal-form-type equations for coupled oscillators. Thus, we would expect the resonance effect to be observable in coupled oscillators that occur in biology, chemistry, mechanics, and electronics (see [9,10] for reviews and extensive bibliographies).

We consider the following nondimensional equations for two mutually coupled identical lasers [1]:

$$\frac{dy_1}{dt} = x_1(1+y_1),$$

$$\frac{dx_1}{dt} = -y_1 - \epsilon x_1(a_1 + by_1) + \epsilon d_2 y_2,$$

$$\frac{dy_2}{dt} = x_2(1+y_2),$$

$$\frac{dx_2}{dt} = -y_2 - \epsilon x_2(a_2 + by_2) + \epsilon d_1 y_1, \tag{1}$$

where x_j and y_j represent deviations from the nonzero steady state of the inversion and intensity of laser j, respectively. $\epsilon \ll 1$ is the ratio of the inversion decay time to the intensity-decay time, and a_j and b are nondimensional constants that take into account both energy-removing dissipation and the energy-supplying pump. The ϵd_k represent the coupling strength of laser k to laser j. If there is a significant time delay in the coupling path, then the coupling term in the equations for the inversion becomes

$$\frac{dx_j}{dt} \sim +\epsilon d_k y_k(t-\tau), \tag{2}$$

where τ is the time delay. The derivation of the nondimensional model and the precise definition of all of the parameters and constants can be found in our earlier works [1,2]. We reiterate that the resonance phenomenon that we will describe can be considered generic to two mutually coupled oscillators such that Eqs. (1) serve as simply an example.

Of particular importance to our work is that we allow for independent control of the coupling constants d_j, and moreover, for Eqs. (1) (without delay) we allowed one of the d_j to be negative; specifically, we fix $d_1 > 0$ and allow $d_2 < 0$ to be the variable control parameter. We find that when $d_2 = d_{2H} \equiv -(a_1 a_2)/d_1$, there is Hopf bifurcation to oscillatory solutions. Then as $|d_2|$ is increased further, there is a singular point $d_2 = d_{2S} \equiv -(a_1 d_1)/a_2$ in the leading-order bifurcation equation such that as $d_2 \to d_{2S}$, the amplitude of the periodic solutions becomes large. This is shown in Fig. 1(a), where the (+) are numerical results and the solid curve is the leading-order bifurcation equation, Eq. (4), which we will describe in the next section; the latter has a pole-type singularity at $d_2 = d_{2S}$. We also show in the inset figures that at the peak of resonance the oscillations are pulsating (in y) and large amplitude, while away from the resonance the oscillations are small and nearly harmonic. One physical interpre-

*FAX: 214-768-2355. tcarr@smu.edu

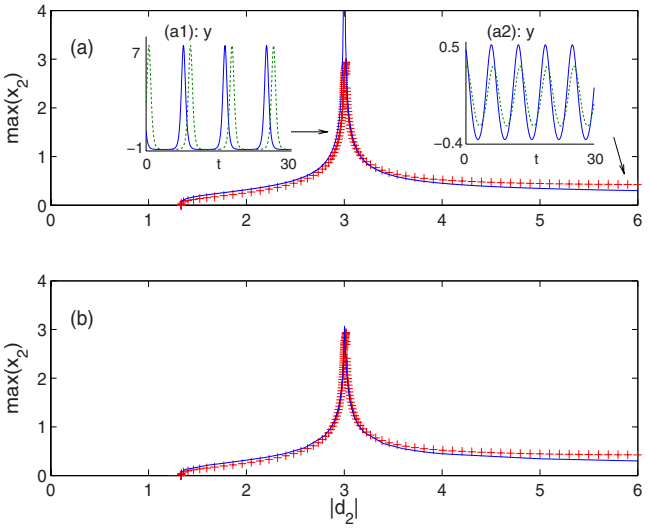

FIG. 1. (Color online) (a) Amplitude of x_2 as a function of $|d_2|$: numerical (+) (AUTO [22]) analytical from Eq. (4) (solid line). Parameter values are $\epsilon=0.001$, $a_1=a_2=2$, $b=1$, and $d_1=3$ so that $d_{2H}=-4/3$ and $d_{2S}=-3$. In the inset (1) we show the pulsating y_j near the peak of the resonance (y_1, dashed line; y_2 solid line), while in inset (a2), y_j is small amplitude and nearly harmonic. (b) Same as (a) except the solid curve results from numerical simulation of Eq. (11).

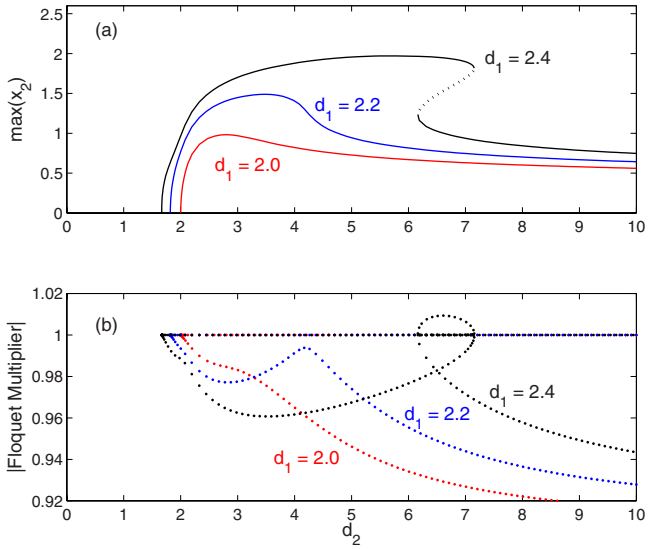

FIG. 2. (Color online) Numerical [23] (a) bifurcation diagram for the amplitude of x_2 and (b) the magnitude of the Floquet multipliers for Eqs. (1) with delay coupling. In (a) the dotted portion of the curve for $d_1=2.4$ represents unstable solutions. Parameter values are $\epsilon=0.01$, $a_1=a_2=2$, $b=1$, and $\tau=\pi$.

tation for the source of the resonance is that the coupling term provides an effective negative damping that cancels with the lasers self-damping, which allows the amplitude to become large; this is suggested by the singularity condition where $|d_2|/d_1=a_1/a2$. In this paper we will show that the resonance also corresponds to matching the nonlinear-amplitude corrections between the slowly evolving phases of each oscillator, which, in essence, corresponds to frequency matching between the oscillators. We then show that by deriving the higher-order nonlinear dissipation terms of the relevant normal-form or averaged equations, the singularity in the bifurcation equation is removed.

The resonance effect continues to be exhibited when coupling terms in Eqs. (1) are modified to include the delay term of Eq. (2). However, in the presence of delay, the bifurcation curve of periodic solutions folds to form intervals in d_2 of bistability, which can be seen in Fig. 2 (see also Fig. 7 of [2]). More generally, multistability of periodic oscillations is a generic feature of systems with delay and has been explored quite extensively in lasers with delay [3–5]. Multistability turns out to be the origin of what we referred to as "discontinuous unfolding" of the bifurcation curve in [2]; there, we found that a small change in the parameter leads to a dramatic change in the bifurcation diagram (see Fig. 7c of [2]). In hindsight, the origin of this distinct qualitative change is obvious; namely, there is a critical value of the coupling such that there is an "imperfect bifurcation" [6,7] and branch "pinch-off" between coexisting branches of solutions. A related phenomenon is the generation of "isolas" [6,8] or isolated branches of solutions that are generated by varying the delay. The second main topic of this paper is to describe the interaction of the coexisting solution branches that lead to the imperfect bifurcations and the isolas.

It is often the case that the main point of interest in the study of coupled oscillators is their degree of synchronization, which implies a focus on the phase- and frequency-locking characteristics of the oscillators. Thus, many investigations focus on coupled-phase oscillators [9,10]. However, a phase-only description is insufficient to describe the amplitude resonance effect and we are required to consider more general evolution equations for both the amplitude and phase. Other amplitude-dependent effects in coupled oscillators include oscillator death and localization. Oscillator death describes the situation when the coupling constants can be tuned such that oscillatory solutions become unstable and the system returns to steady-state behavior; this has been investigated for systems with instantaneous coupling [9,11,12] as well as for delayed coupling [13–15]. Localized solutions refer to when the amplitudes of the different oscillators have different orders of magnitude and has been studied in [16,17].

In the next section we will consider the analysis of Eqs. (1) without delay coupling. We will show that including the effect of nonlinear dissipation removes the singularity that appeared in the leading-order bifurcation equation. In Sec. III we will use numerical continuation to explore the system with delayed coupling and track how the bifurcation diagram deforms as a function of the parameters. In particular, we will track disconnect bifurcation curves that result from imperfect bifurcations of the curve that originates at the Hopf bifurcation. We will finish with a brief discussion in Sec. IV.

II. REMOVAL OF RESONANCE SINGULARITY

We will first review the results from [1], where we used the method of multiple scales [18] to study the properties of the small-amplitude oscillatory solutions to Eqs. (1) that

emerge when $|d_2|>|d_{2H}|$. We derived the coupled Stuart-Landau equations

$$\frac{dA_j}{dT} = -\frac{1}{2}a_jA_j - \frac{1}{6}i|A_j|^2A_j - \frac{1}{2}id_kA_k \tag{3}$$

for $j=1,2$ and $k=2,1$, and where $x_j \approx \epsilon^{1/2}A_j(T)\exp(it)+\text{c.c.}$ and $T=\epsilon t$ ("c.c." stands for complex conjugate). Thus, the complex function $A_j(T)=R_j(T)e^{i\theta_j(T)}$ determines the slowly evolving amplitudes $R_j(T)$ and the phases $\theta_j(T)$. The x_j and y_j are periodic if the amplitudes and phase difference $(\theta_2-\theta_1)$ are constant with respect to the slow-time T (i.e., their derivatives with respect to T are zero). The resulting algebraic equations can be solved to determine the bifurcation equation for R_2, which is given by [Eq. (17) in [1]]

$$R_2^4 = 9(a_1+a_2)^2\frac{\left(\frac{d_2}{d_{2H}}-1\right)}{\left(\frac{d_2}{d_{2S}}-1\right)^2},$$

$$d_{2H} = -\frac{a^2}{d_1}, \quad d_{2S} = -d_1. \tag{4}$$

The amplitude R_1 and the phase different ψ are functions of R_2 [see Eq. (18) in [1]]. The denominator of Eq. (4) is zero when $d_2=d_{2S}$, which indicates that the amplitude of the periodic oscillations becomes large when $d_2 \to d_{2S}$. The numerical resonance peak and the singular bifurcation result are shown in Figs. 1(a).

To better understand the coupling resonance, we consider the following generic amplitude equations corresponding to two nearly identical coupled oscillators with asymmetric coupling:

$$A_{jT} = (a_{j1}+ib_1)A_j + (a_2+ib_2)A_j|A_j|^2 + (a_3+ib_3)A_j|A_j|^4 + \cdots + id_kf(A_k,A_j) \tag{5}$$

for $j=1,2$ and $k=2,1$. The two oscillators differ only in their linear dissipation, represented by a_{j1}, and the asymmetric coupling in that d_2 does not, in general, equal d_1.

We first consider when there is only linear damping and linear coupling. Specifically, we assume that $a_{j1}\neq 0$ and $a_l=0$, $l=2,3,\ldots$, such that the only coefficient with nonzero real part is the linear term $A_{jT}\sim a_1A_j$. Additionally, we assume that the coupling function is similar to Eq. (3), where $f(A_k,A_j)=A_k$. In the Appendix we show that in this case there will always be a singular point such that when $d_2 \to d_{2S}$ the amplitude becomes unbounded; specifically, in Eq. (A9) we see that the amplitude of periodic solutions will be singular when $d_2=d_{2S}$. Notice that in Eq. (A4) when $d_2=d_{2S}$, then $R_1=R_2$. Then in Eq. (A3) for ψ_T the amplitude dependence of the slow phase is removed except for the coupling terms. Thus, in general, the singularity, and hence the resonance, results from matching the amplitudes such that the nonlinear amplitude terms vanish from the phase equation, which corresponds to frequency matching.

To remove the singularity from the bifurcation equation we must include the effect of the nonlinear dissipation—i.e., the real coefficients in Eq. (5); it will suffice to consider $a_{j1}=0$ and $a_2\neq 0$ and ignore all of the nonlinear terms of power 5 or greater. Thus, we consider

$$A_{jT} = (a_2+ib_2)A_j|A_j|^2 + id_kA_k \tag{6}$$

for $j=1,2$ and $k=2,1$. When we look for steady-state solutions, we find that

$$R_1^4 = \rho R_2^4, \quad \rho = -\frac{d_2}{d_1} \tag{7}$$

and

$$R_2^4 = \frac{d_1^2\rho^{1/2}(1+\rho^{1/2})^2}{b_2^2(1-\rho^{1/2})^2 + a_2^2(1+\rho^{1/2})^2}. \tag{8}$$

Even when $\rho=1$ the denominator is strictly positive for $a_2\neq 0$, so there will be no singularity. If $a_2=0$, then we would consider the real coefficient a_3 of the quintic nonlinearity, which would remove the singularity. Thus, we see that the singularity in the bifurcation equation that results from frequency matching is removed by taking into account higher-order nonlinear dissipation.

Unfortunately, for our specific problem, when we look for small-amplitude $O(\epsilon^{1/2})$ solutions using the method of multiple scales, we find that both $a_2=0$ and $a_3=0$. Continuing the analysis to even higher order in ϵ becomes algebraically difficult. Instead, we have taken an alternative approach to find the relevant Stuart-Landua amplitude equations. We begin by looking for $O(1)$ amplitude solutions to Eqs. (1) formulated in terms of the energy and phase [16,19]. This allows us to derive the following integral constraint, which ensures a constant value for the energy of oscillatory solutions:

$$\int_0^P (-ax_{j0}^2 + d_kx_{j0}y_{k0})dt = 0, \tag{9}$$

where P is the period of the oscillations. The x_{j0} and y_{j0} are the $\epsilon=0$ solutions to Eqs. (1), the latter given by

$$\frac{dy_{j0}}{dt} = x_{j0}(1+y_{j0}), \quad \frac{dx_{j0}}{dt} = -y_{j0}. \tag{10}$$

The key idea of our alternative approach is that in the limit of small-amplitude solutions, Eq. (9) should produce the same condition for periodic solutions as we found from Eqs. (3) and (5).

To evaluate the integrals in Eq. (9) we need to solve Eq. (10), which does not yield an exact solution. Instead, we find approximations for x_{j0} and y_{j0} in the limit of small amplitude by using the Poincaré-Linstedt method (strained coordinates) [18]. Specifically, we let $x_{j0}=\eta x_{j1}+O(\eta^2)$ and similarly for y_{j0}, where $\eta \ll 1$ is a measure of the small size of x_{j0}. We also rescale time according to $s=(1+\eta^2\omega_2+\cdots)t$ and solve for ω_2. The solutions for x_{j0} and y_{j0} are used to evaluate the integrals in Eq. (9). The integral on x_j^2 will determine all the real coefficients, i.e.—the dissipation—in Eq. (5). The integral on x_jy_k determines the coupling term in Eq. (5). What remains to be determined are the imaginary coefficients in

Eq. (5). These correspond to the amplitude-dependent frequency correction ω_2, which is determined by the Poincaré-Linstedt analysis.

In sum, the coefficients a_j in Eq. (5) are determined by the integral on x_{j0}^2, the functional form of the coupling term is determined from the integral on $x_{j0}y_{k0}$, and the coefficients b_j are determined by the amplitude-dependent frequency correction. The result is

$$A_{jT} = -\frac{a_j}{2}A_j - \left(\epsilon\frac{a_j}{9} + \frac{i}{6}\right)A_j|A_j|^2 - \frac{i}{2}d_kA_k\left(1 - \epsilon\frac{1}{6}|A_k|^2 + \epsilon\frac{1}{9}A_j^*A_k\right) \quad (11)$$

for $j=1,2$ and $k=2,1$. The introduction of the parameter ϵ on some coefficients indicates that these terms would be generated by higher-order terms in the more systematic multiple-scale approach. We note that the $O(1)$ terms in Eq. (11) are the same as those that appear in Eq. (3). We will validate the $O(\epsilon)$ terms in Eq. (11) by comparing the predicted amplitudes to simulations of the original model.

By formulating the solvability condition based on the leading-order nonlinear problem given by Eq. (10), the coupling term becomes nonlinear function of the amplitudes. The steady-state conditions for the amplitudes R_j that result from Eq. (11) are a pair of nonlinear algebraic equations without a closed-form solution and require numerical evaluation. Instead, we have chosen to simulate Eq. (11) directly. In Fig. 1(b) we compare the numerical bifurcation diagram of the original model, Eq. (1), to the numerical bifurcation diagram generated by Eq. (11) and obtain an excellent fit. The bifurcation curves match well away from the resonance peak and agree to within 5% at the resonance peak. We have also confirmed that both the nonlinear dissipation and the nonlinear coupling terms in Eq. (11) are necessary to obtain good agreement; more specifically, eliminating the terms that depend on A_j from the coupling reduces the quality of fit.

Finally, we note that the coupling coefficient in all the amplitude equations that we consider is imaginary. This is motivated by the fact that the incoherent coupling [5] considered in Eq. (1) leads to the purely imaginary coupling coefficient in Eq. (3). However, we note that the bifurcation results of the Appendix and in this section are unchanged if the coupling coefficient is strictly real and are qualitatively unchanged but algebraically more complicated if they are complex.

III. RESONANCE DUE TO DELAY

We now consider Eq. (1) in the presence of delay where the coupling term is given by Eq. (2). With delay the resonance peak occurs when both coupling constants are of the same sign. The opposite sign coupling used when the coupling is instantaneous provides the necessary phase shift such that for small-amplitude harmonic solutions it is equivalent to a time delay of half the period (see the Appendix of [2]). In [2] we used negative coupling to be consistent with the experimental setup that we were considering. In the present paper we will use positive coupling because the numerical results are easier to display and describe, while being qualitatively equivalent. For small-amplitude harmonic oscillations, the difference in the sign of the coupling is of little consequence because the Hopf bifurcation point and the amplitudes depend upon the product of the coupling constants. However, for large-amplitude oscillations y_j is pulsating, so the coupling signal is not invariant with respect to the sign of the coupling.

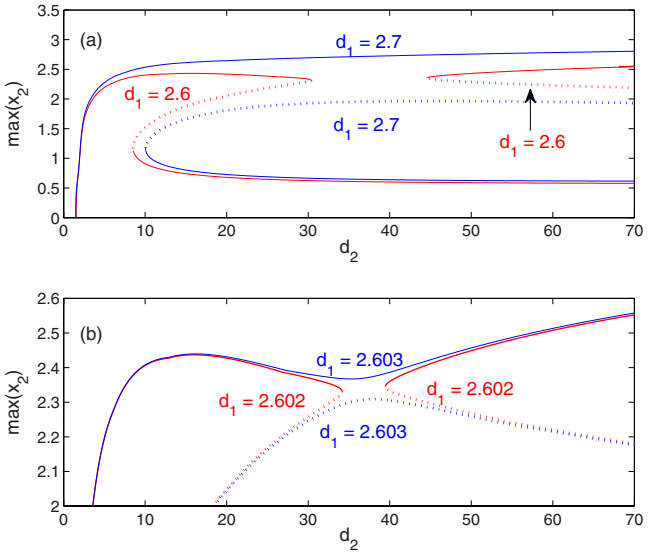

FIG. 3. (Color online) (a) Numerical bifurcation curves for $d_1=2.6$ and $d_1=2.7$. Solid and dashed curves represent stable and unstable solutions, respectively. Other parameters are the same as in Fig. 2. (b) d_1 is close to the critical value for an imperfect bifurcation.

Without delay the resonance peak is singled valued; that is, for every value of d_2 there is a single value for the amplitude of periodic solutions. However, with delay we find that d_1 can be tuned such that the resonance peak folds to form an interval in d_2 when there is bistability, as shown in Fig. 2; the fold is reminiscent of the resonance that occurs in forced nonlinear oscillators [20].

In [2] we reported that when d_1 was increased further there was a "discontinuous" change in bifurcation curve. However, in addition to the original branch of periodic solutions that emanated from the Hopf bifurcation there are other disconnect branches of periodic solutions. By tracking the additional disconnect solution branches we can follow the continuous deformation of the bifurcation curves as d_1 is varied. To begin, in Fig. 3(a) we see that for $d_1=2.6$ there is a second branch of solutions for larger d_2 that is to the right of the folded resonance peak; it appears via a saddle-node bifurcation at $d_2 \approx 45$. Thus, the system is monostable just after the Hopf bifurcation, is bistable between the two limit points of the original bifurcation curve, becomes monostable for d_2 greater than the right-hand limit point at $d_2 \approx 30$, and becomes bistable again when the second branch of solutions appears at the $d_2 \approx 45$.

Now consider when $d_1=2.7$ in Fig. 3(a) in which there is no resonance peak. In this case, the bifurcation curve that originated at the Hopf bifurcation point does not fold and remains at $O(1)$ amplitudes. However, there is a lower folded

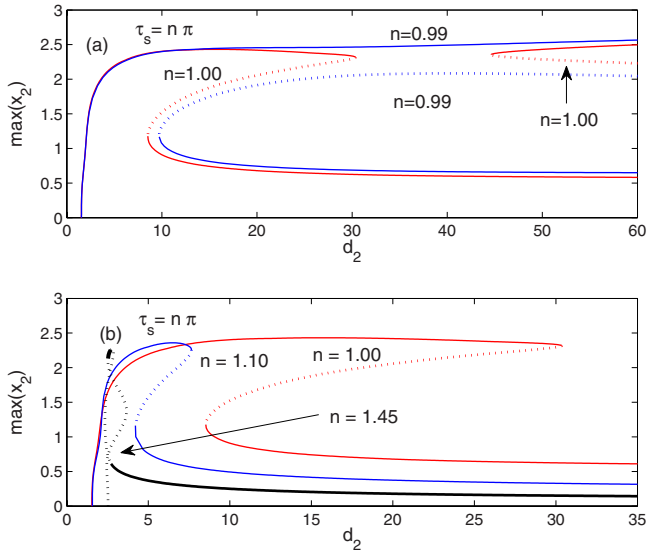

FIG. 4. (Color online) (a) Numerical bifurcation diagram as τ increases through the imperfect bifurcation. Solid (dashed) curves represent stable (unstable) solutions. $d_1=2.6$, while other parameters are the same as in Fig. 2. (b) As τ is increased further, the interval of bistability decreases.

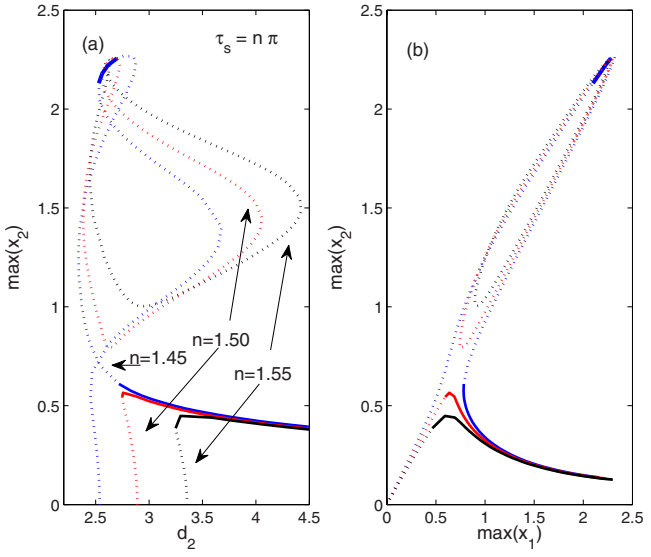

FIG. 5. (Color online) Numerical bifurcation diagrams as d_2 is varied shown in the (a) $(d_2,\max(x_1))$ and (b) $(\max(x_1),\max(x_2))$ planes. Solid (dashed) curves represent stable (unstable) solutions. $d_1=2.6$, while other parameters are the same as in Fig. 2.

branch of solutions that appears via a saddle-node bifurcation when $d_2\approx 11$. The upper portion of the folded branch is unstable, while the lower portion is stable.

In Fig. 3(b) we track the deformation of the bifurcation curves as d_1 is decreased from 2.7 to 2.6. As d_1 decreases, the amplitude of the original branch of solutions decreases, while the upper part of the folded branch increases. When $d_1=2.603$ the two curves almost merge at $d_2\approx 36$. When $d_1=2.602$ the upper and lower bifurcation curves have merged and then been "pinched off" such that there are now left- and right-hand limit points and left- and right-side disconnected bifurcation branches. The merging and pinching of the bifurcation curves that we have described is an example of an imperfect or broken bifurcation [6,7].

In Fig. 4 we track the changes in the bifurcation curves as we vary the delay time τ. In Fig. 4(a) we see that as we increase the delay from less than $\tau=\pi$, the upper and lower branches of solutions pass through an imperfect bifurcation to form a folded resonance peak on the left and a disconnected branch of solutions on the right. As τ is increased further, the disconnected branch moves to the right such that the limit point occurs for higher values of d_2. In Fig. 4(b) we focus on the bistable resonance peak and follow its deformation as τ is increased further. We see that as τ increases, the interval of bistability decreases. For $\tau=1.45\pi/2$ the bifurcation curve intersects itself in this two-dimensional projection of the more general bifurcation curve.

In Fig. 5 we again consider the case when $\tau=1.45$. In Fig. 5(b) we show the projection of the bifurcation curve in the $(\max(x_1),\max(x_2))$ plane and see that the bifurcation curve does not actually intersect itself. Notice that solutions that originate at the Hopf bifurcation point are unstable. As d_2 is increased from below the Hopf bifurcation point to above, the system will jump from the now unstable steady state to the small interval of stable oscillations where $\max(x_1)\approx 2.25$. For larger values of d_2 the stable part of the branch of solutions occurs for smaller amplitudes when $\max(x_1)\approx 0.5$.

When the delay is increased from $\tau=1.45\pi/2$ to $\tau=1.5\pi/2$, an imperfect bifurcation occurs such that the resonance peak "pinches off" to form an isola [6,8]—i.e., an isolated branch of solutions—which in this case is unstable. Thus, for the cases $\tau=1.5\pi/2$ and $\tau=1.55\pi/2$ that are shown in Fig. 5, when d_2 is increased from below to above the Hopf bifurcation point the system will jump to periodic solutions with amplitude $\max(x_1)\approx 0.5$.

IV. DISCUSSION

The coupling-induced resonance we describe is a generic property of the very-well-known Stuart-Landau equations and should be observable in any coupled-oscillator system where the former are the relevant normal-form equations. For systems described by the Stuart-Landau equations the amplitude remains a dynamically evolving variable; in contrast, for limit-cycle oscillators, the described phase equations, the amplitude is fixed and there will not be a coupling-resonance affect. For instantaneous coupling the only novelties we introduce are to allow the coupling coefficients to be individually tunable and of opposite sign. With delayed coupling the resonance is exhibited for same-sign coupling. In [1] we also show that the resonance can be exhibited in systems of more than two coupled oscillators with appropriate tuning of the coupling coefficients.

Observation of the resonance may require very precise control over the system parameters because it occurs over a relatively small interval of the coupling coefficients. For example, in the laser experiments of [21] we could not control the coupling strength with fine enough resolution and the resonance was not observed. Other experimental systems of

coupled oscillators may allow for better tuning of the coupling strength and, hence, allow for the observation and potential exploitation of the resonance phenomena.

Our previous analysis located the resonance peak as a singular point in the bifurcation equation. In this paper we show that accounting for nonlinear dissipation is sufficient to remove the singularity from the analytical results. For our particular example we needed to change our analytical approach to an energy-phase formulation that allowed for larger amplitude solutions; in this way, we could derive the required higher-order contributions to the amplitude equations.

We also show that the resonance results when the oscillator amplitudes are tuned such that the amplitude-dependent frequency corrections of each oscillator are matched; this observation is consistent with the typical notion of resonance in periodically forced systems, where the forcing frequency is matched to the natural frequency of the oscillator. We may also think of the resonance as resulting from the signal of the coupling term canceling with the oscillator's self-dissipation.

In our analysis we considered nearly identical oscillators. In general, allowing for additional small detunings of the other oscillator coefficients merely complicates the analysis, but the resonance effect can still be observed. We note that linear frequency detuning in the case of instantaneous coupling [$b_1 \to b_{1j}$ in Eq. (5)] can shift the Hopf bifurcation point and the singular point, and can significantly distort the bifurcation curve; the effect is similar to changing the delay when there is delayed coupling. We have focused on the case when the resonance appears near the Hopf bifurcation point and have not tried to investigate the situation when the resonance might interfere with secondary bifurcations that occur for larger coupling [1].

APPENDIX: CORRECTIONS TO PHASE

We consider the special case of Eq. (5), but with only linear damping and linear coupling. In this case, we have

$$A_{jT} = a_{j1}A_j + ib_2A_j|A_j|^2 + ib_3A_j|A_j|^4 + \cdots + id_kA_k, \tag{A1}$$

which decomposes to amplitude and phase equations as

$$R_{jT} = a_{j1}R_j \mp d_kR_k \sin\psi, \tag{A2}$$

$$\psi_T = \sum_{l=2} b_l[R_2^{2(l-1)} - R_1^{2(l-1)}] + \left(d_1\frac{R_1}{R_2} - d_2\frac{R_2}{R_1}\right)\cos\psi \tag{A3}$$

[take the $(-)$ if $j=1$, $k=2$ and the $(+)$ if $j=2$, $k=1$]. Periodic oscillatory solutions to the original oscillator model correspond to steady-state solutions of the amplitude equations, where the time derivative equals zero. We find that

$$R_1^2 = -\frac{a_{21}d_2}{a_{11}d_1}R_2^2 \tag{A4}$$

and $\psi=\psi(R_2)$ is a fixed function of the amplitude. Then using $\cos^2\psi+\sin^2\psi=1$ we have

$$-\frac{[\Sigma_{l=2}b_lS_2^{l-1}(1-\rho^{l-1})]^2}{4d_1d_2} - \frac{a_{11}a_{21}}{d_1d_2} = 1, \tag{A5}$$

where $S_j=R_j^2$ and $\rho=-\frac{a_{21}d_2}{a_{11}d_1}$. The last result can be simplified to

$$\left[\sum_{l=2} b_lS_2^{l-1}(1-\rho^{l-1})\right]^2 = -4(a_{11}a_{21}+d_1d_2). \tag{A6}$$

So that the right-hand side is positive, we require that $d_2 \leqslant -(a_{11}a_{21})/d_1$, which corresponds to increasing $|d_2|$ beyond the Hopf bifurcation point.

The following two properties allow us to simplify Eq. (A6):

$$S_2^{l-1} = S_2S_2^{l-2}, \tag{A7}$$

$$1-\rho^{l-1} = (1-\rho)(1+\rho+\rho^2+\cdots+\rho^{l-2}) = (1-\rho)\sum_{m=0}^{l-2}\rho^m. \tag{A8}$$

After some additional algebra Eq. (A6) becomes

$$S_2^2\left[\sum_{l=0}\left(b_{l+2}S_2^l\sum_{m=0}^{l}\rho^m\right)\right]^2 = \frac{-4(a_{11}a_{21}+d_1d_2)}{(1-\rho)^2}. \tag{A9}$$

Equation (A9) is the bifurcation equation that describes the amplitude $S_2=R_2^2$ as a function of the parameters.

For the case that $b_2\neq 0$ but $b_j=0$, $j=3,4,\ldots$, we recover the previous bifurcation equation

$$S_2^2 = \frac{-4(a_{11}a_{21}+d_1d_2)}{b_2^2(1-\rho)^2}. \tag{A10}$$

In general, we see that the bifurcation equation will always have the term

$$1-\rho = 1+\frac{a_{21}d_2}{a_{11}d_1}, \tag{A11}$$

in the denominator for S_2, which is singular when $d_2=-(a_{11}d_1)/a_{21}$.

[1] T. W. Carr, M. L. Taylor, and I. B. Schwartz, Physica D **215**, 152 (2006).
[2] T. W. Carr, I. B. Schwartz, M. Y. Kim, and R. Roy, SIAM J. Appl. Dyn. Syst. **5**, 699 (2006).
[3] D. Pieroux and P. Mandel, Phys. Rev. E **67**, 056213 (2003).
[4] D. Pieroux, T. Erneux, A. Gavrielides, and V. Kovanis, SIAM J. Appl. Math. **61**, 966 (2000).
[5] D. Pieroux, T. Erneux, and K. Otsuka, Phys. Rev. A **50**, 1822 (1994).
[6] G. Ioos and D. D. Joseph, *Elementary Stability and Bifurcation Theory* (Springer-Verlag, New York, 1980).
[7] B. J. Matkowski and E. L. Reiss, SIAM J. Appl. Math. **33**, 230 (1977).
[8] D. Dellwo, H. B. Keller, B. J. Matkowski, and E. L. Reiss, SIAM J. Appl. Math. **42**, 956 (1982).
[9] D. G. Aronson, G. B. Ermentrout, and N. Kopell, Physica D **41**, 403 (1990).
[10] S. H. Strogatz, Physica D **143**, 1 (2000).
[11] B. Ermentrout and N. Koppell, SIAM J. Appl. Math. **50**, 125 (1990).
[12] R. Karnatak, R. Ramaswamy, and A. Prasad, Phys. Rev. E **76**, 035201(R) (2007).
[13] D. V. R. Reddy, A. Sen, and G. L. Johnston, Phys. Rev. Lett. **80**, 5109 (1998).
[14] D. V. R. Reddy, A. Sen, and G. L. Johnston, Physica D **129**, 15 (1999).
[15] R. Vicente, S. Tang, J. Mulet, C. R. Mirasso, and J. M. Liu, Phys. Rev. E **73**, 047201 (2006).
[16] R. Kuske and T. Erneux, Opt. Commun. **139**, 125 (1997).
[17] R. Kuske and T. Erneux, Eur. J. Appl. Math. **8**, 389 (1997).
[18] J. Kevorkian and J. D. Cole, *Multiple Scale and Singular Perturbation Methods* (Springer-Verlag, New York, 1996).
[19] T. W. Carr, L. Billings, I. B. Schwartz, and I. Triandaf, Physica D **147**, 59 (2000).
[20] A. Nayfeh and D. T. Mook, *Nonlinear Oscillations* (Wiley, New York, 1979).
[21] M.-Y. Kim, R. Roy, J. L. Aron, T. W. Carr, and I. B. Schwartz, Phys. Rev. Lett. **94**, 088101 (2005).
[22] E. J. Doedel, R. C. Paffenroth, A. R. Champneys, T. F. Fairgrieve, Yu. A. Kuznetsov, B. Sandstede, and X. Wang, AUTO 2000, continuation and bifurcation software for ordinary differential equations (with homcont), California Institute of Technology, 2001.
[23] K. Engelborghs, T. Luzyanina, and G. Samaey, DDE-BIFTOOL v. 2.00 user manual, a Matlab package for bifurcation analysis of delay differential equations, K. U. Leuven, 2001.